JOURNAL OF CATALYSIS 134, 629–643 (1992)

Influence of Catalyst Parameters and Operational Variables on the Photocatalytic Cleavage of Water

KYRIAKI E. KARAKITSOU AND XENOPHON E. VERYKIOS

Institute of Chemical Engineering and High Temperature Chemical Processes, and Department of Chemical Engineering, University of Patras, GR 26110 Patras, Greece

Received December 21, 1990; revised September 24, 1991

The photocatalytic cleavage of water over Pt–RuO_2/TiO_2 catalysts under illumination in the near UV (250–400 nm) is investigated in a batch and in a semicontinuous flow photoreactor cell. The effects of operational variables and parameters related to chemical and physical characteristics of the catalyst on the rate of hydrogen production are investigated. It is shown that the rate of the process is insensitive to the details of surface structure of Pt; the rate exhibits a weak maximum at a Pt loading of 0.5 wt% and is independent of Pt loading when this exceeds 1 wt %. The rate of H_2 production is strongly dependent on the pH of the slurry, increasing significantly at pH levels higher than 10. The rate was also observed to be a linear function of the intensity of illumination in the near UV. © 1992 Academic Press, Inc.

INTRODUCTION

The possibility of converting solar energy into chemical energy that can be easily stored and transported has initiated considerable research activity in the area of photochemical water cleavage. Hydrogen evolution in sacrificial as well as cyclic photoinduced processes (*1*) seems to be the simplest and most attractive method for energy production utilizing solar radiation. Hydrogen has the added advantage of being an environmentally clean fuel.

Of the various photocatalytic systems and processes (*2*) that have been developed, those employing semiconducting materials in massive or highly dispersed form as photocatalysts seem to be the most attractive. The reaction of photochemical water cleavage over semiconducting materials under irradiation with light of energy higher than their band-gap energy can be represented by the following simplified scheme:

$$\mathrm{MO} \xrightarrow{h\nu} e^- + h^+ \qquad (1)$$

$$2e^- + 2\mathrm{H_2O} \rightarrow \mathrm{H_2} + 2\mathrm{OH^-} \qquad (2)$$

$$4h^+ + 2\mathrm{H_2O} \rightarrow \mathrm{O_2} + 4\mathrm{H^+}. \qquad (3)$$

However, due to high overpotentials developing and due to the multielectron transfer requirements, in the absence of suitable redox catalysts, reactions (2) and (3) either do not occur or occur with low efficiency.

Potential semiconductor materials for this process must possess certain characteristics such as suitable band-gap energies, stability toward photocorrosion, and suitable physical characteristics that enable them to act as catalysts for H_2 and O_2 evolution. Various semiconducting oxides have been investigated for this purpose, such as CdS (*3*), $K_4Nb_6O_{17}$ (*4*), $SrTiO_3$ (*5, 6*), and TiO_2 (*7–10, 12*), loaded with suitable metals and metal oxides. By far the most suitable materials seem to be TiO_2 and $SrTiO_3$ because of their high stability toward photocorrosion and their favorable band-gap energies. Attempts to improve the performance of these materials by surface doping have also been reported (*13–16*).

The evolution of hydrogen by the water cleavage reaction is assisted by the presence of metal crystallites dispersed on the surface of the semiconductors. The electrons generated in the conduction band of the semiconducting oxides under illumination are trans-

0021-9517/92 $3.00

ported to the metal particles, thus retarding the possibility of their recombination with positive holes of the valence band. The best metal for this purpose has been shown to be Pt (*2, 9–11*), although other metals such as Rh (*17, 18*), Pd (*19*), and Ru (*17*) have also been investigated. The performance of the Pt/TiO_2 catalyst can be improved by addition of RuO_2 (*20*) whose function might be to scavenge the holes from the valence band of the semiconductor. Thus $Pt–RuO_2/TiO_2$ is an effective bifunctional catalytic system for water splitting and H_2 production under UV irradiation.

In the present investigation, the $Pt–RuO_2/TiO_2$ catalyst is employed to investigate the influence of various parameters related to the structure of the catalyst and various operating variables on the rate of H_2 evolution under UV irradiation. An attempt is also made to develop an expression for the intrinsic rate of H_2 production, which may assist in unifying the literature in this field and may provide a common denominator for comparison of the performance of different catalyst formulations. Operating parameters under which intrinsic rates can be obtained are also defined.

EXPERIMENTAL

(*a*) *Catalyst Preparation*

The semiconductor employed as catalyst carrier in the present study was TiO_2 (Degussa P25), used as received. Two types of catalysts were prepared: monofunctional, containing Pt only or RuO_2 only; and bifunctional, containing both Pt and RuO_2. RuO_2/TiO_2 was prepared by the method of incipient wetness impregnation. TiO_2 powder was added to an aqueous solution of $RuCl_3 \cdot 3H_2O$ (obtained from Alfa Products) of sufficient concentration (0.04 *M*) so as to obtain a RuO_2 loading of 1 wt% in the product. The slurry was heated to 80°C and stirred until nearly all the water evaporated. The resulting paste was dried at 100°C for 24 h and was subsequently calcined at 400°C for 8 h to oxidize Ru(III) to RuO_2. This method of loading RuO_2 to TiO_2 is similar to that described by other investigators (*16, 21, 22*), although different preparation methods have also been reported (*15, 20*).

Platinization of TiO_2 or RuO_2/TiO_2 was achieved by three methods: by incipient wetness impregnation (method A), by Pt-citrate sol formation (method B), and by photoplatinization (method C). In the method of incipient wetness impregnation, TiO_2 or RuO_2/TiO_2 (prepared as described above) were added to aqueous solutions of H_2PtCl_6 (obtained from Alfa Products) of appropriate concentration so as to obtain a final product with the desired Pt loading. Water was evaporated at low temperature while the slurry was continuously stirred. The resulting paste was dried at 100°C for 24 h. The dried powder was placed into a continuous flow system and was heated to 200°C in the presence of N_2 flow (80 cm^3/min), followed by hydrogen flow (80 cm^3/min) at the same temperature for 2 h after which it was cooled under nitrogen flow. In certain cases the reduction was conducted at 400 or 500°C, following the same procedure.

In the preparation procedure involving Pt–citrate sol formation, the method described by Mills (*23*) was followed. A Pt–citrate sol was prepared by refluxing, for 4 h and at temperatures up to 90°C, a solution containing 1.5 ml of a 0.05 *M* H_2PtCl_6 solution, 30 ml of a 1 wt% sodium citrate solution, and 120 ml of H_2O. One gram of TiO_2 and 5.8 g of NaCl were added to 50 ml of the resulting Pt–sol. The destabilization of the sol was followed by Pt precipitation. The sample was filtered, washed with distilled water, and dried in air. A 0.5% Pt/TiO_2 catalyst was thus prepared. A 0.5% Pt–1% RuO_2/TiO_2 and a 1% Pt–1% RuO_2/TiO_2 catalyst were also prepared following the same procedure.

Following the photoplatinization procedure, Pt was loaded on the 1% RuO_2/TiO_2 particles by photoreduction of Pt(IV) without any sacrificial agents (*21, 23*). A standard solution of H_2PtCl_6, 0.25 ml, was added to a suspension containing 500 mg of 1%

RuO_2/TiO_2 in 40 ml of water. The suspension was placed in the reaction cell of the photolysis apparatus and it was irradiated for approximately 1 h under continuous N_2 flow. The solid was filtered, washed with distilled water, and dried in air. The resulting catalyst contained 0.5% Pt.

(b) Catalyst Characterization

The catalysts employed in the present investigation were characterized in terms of total surface area using the BET method with N_2 adsorption at liquid nitrogen temperature and in terms of free metallic (Pt) area, degree of Pt dispersion, and average size of the Pt crystallites employing selective chemisorption of H_2 at room temperature. The samples used in H_2 chemisorption did not contain any RuO_2 in order to avoid complications arising from H_2 adsorption on RuO_2 surfaces. It is assumed that the presence of RuO_2 in the catalyst formulations did not influence the dispersion of Pt.

Hydrogen uptakes were determined in a constant volume, high-vacuum apparatus (Micromeritics Accusorb 2100 E). Prior to adsorption measurements the catalyst samples were evacuated under heating at 200°C for 2 h, exposed to H_2 at a pressure of 100 Torr for 2 h, kept in a dynamic vacuum at 250°C for approximately 10 h, and cooled to room temperature under vacuum. Hydrogen uptakes were determined at H_2 equilibrium pressures between 5 and 200 Torr. The volume of H_2 adsorbed at monolayer coverage was obtained by extrapolation of the linear portions of the adsorption isotherms to zero pressure. Small uptakes by the support were accounted for.

(c) Determination of H_2 Production Rates

Hydrogen production rates were determined using an experimental apparatus that consisted of a photoreactor, a xenon lamp with a power supply system, a regulated nitrogen supply system, and an on-line gas chromatograph with a reporting integrator. The photoreactor is a quartz cell with optically flat entry and exit windows for the light. The cell has three inlets/outlets, two of which are closed with glass stopcocks and the third closed with a septum through which samples can be taken with a gas syringe. The cell inlet terminates in a fritted glass section through which gases can be dispersed. The cell reactor can be operated either in a batch or in a semicontinuous mode by regulated nitrogen flow through the cell. The water volume was invariably 40 ml and the gas-phase volume 150 ml.

Continuous illumination was carried out with either a 1000-W Xe lamp or a 450-W Xe lamp (Osram) whose intensity could be varied within limits. Both lamps have outputs at wavelengths above 250 nm. However, radiation above 400 nm was filtered out with a UV-transmitting visible absorbing filter. A water filter was also used to remove IR radiation. The lamp was controlled and regulated by a power supply (Oriel Model 66024).

The experimental procedure involved adjustment of the pH of the solution to the desired level by addition of appropriate quantities of NaOH or HCl, addition of a preweighed amount of catalyst, followed by N_2 purging under continuous stirring so as to remove dissolved oxygen. After this procedure, the slurry was exposed to light under continuous stirring. For batch experiments, all entry and exit ports were closed and samples were taken periodically through the septum with a gas syringe. For semicontinuous experiments a N_2 flow of 45 cm^3/min was directed into the cell and N_2 was dispersed into the solution through the glass frit. The outlet line was connected to a gas chromatograph through a gas sampling valve. Samples were periodically analyzed and the N_2 flow was continuously monitored.

Hydrogen concentration in the gas phase of the cell was determined by gas chromatographic analysis using a Shimadju GC (Model 9A) equipped with a thermal conductivity detector and a reporting inte-

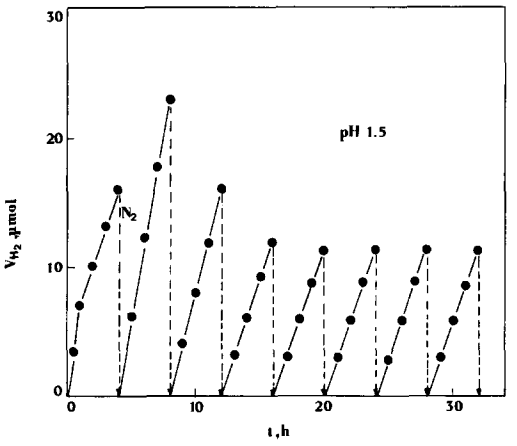

FIG. 1. Typical profile of volume of H_2 produced with respect to time in a batch photoreactor operation using the 0.5% Pt–1% RuO_2/TiO_2 catalyst at a pH of 1.5.

grator. A Carbosieve column ($\frac{1}{8}$ in × 10 ft), maintained at 50°C was used to separate H_2. Nitrogen was used as the carrier gas.

Several reproducibility tests were performed with various catalysts. In all cases, the uncertainty in the measurements of H_2 production rates was found to be less than 5%. Furthermore, the operation of the photoreactor was tested periodically using a standard catalyst under standard conditions.

RESULTS AND DISCUSSION

(*a*) *Batch versus Semicontinuous Experiments*

A typical profile of volume of hydrogen produced with respect to time obtained from a batch photoreactor operation is shown in Fig. 1. The results shown in Fig. 1 were obtained employing the 0.5% Pt–1% RuO_2/TiO_2 catalyst prepared by the incipient wetness impregnation technique and the experiment was conducted at a pH of 1.5. The amount of H_2 accumulating in the gas phase over the slurry increases linearly with time. The vertical dashed lines indicate flushing with N_2 to remove the accumulated H_2. It is apparent that the rate of hydrogen production, which is the slope of the lines of Fig. 1, changes from cycle to cycle, and reaches a steady value after approximately 5 cycles or 20 h of illumination. This behavior is typical of all catalysts used in this study.

The mean rate of hydrogen production, as obtained from plots similar to that of Fig. 1, as a function of mean cycle time is shown in Fig. 2a. The instantaneous rate of hydrogen production in a semicontinuous operation, under otherwise identical conditions, as a function of time is shown in Fig. 2b. These experiments were also conducted with the 0.5% Pt–1% RuO_2 catalyst prepared by method A at pH 1.5 and 13. It is apparent that the dynamic behavior of the two modes of operation differs significantly. In the batch mode of operation, the rate of hydrogen production initially decreases and then rises to a maximum after which it stabilizes after many hours of illumination. On the other hand, in the case of the semicontinuous operation, the rate initially increases rapidly, goes through a narrow maximum and stabilizes,within a short period of time, at a value somewhat higher than that of the batch reactor operation. Qualitatively identical "dynamic" behavior of the batch and semicontinuous reactor operation has been observed with all catalyst formulations. Differences in the dynamic behavior with respect to catalyst particle size are discussed below in Section (e).

Differences in the dynamic behavior of the two reactor operations might be due to different hydrogen concentrations in the liquid phase. As shown in Fig. 2 (see also Section (e)), the rate of hydrogen production is quite sensitive to the pH of the solution. The presence or absence of dissolved hydrogen in the solution could affect the rate of interaction of TiO_2 with the solution, primarily the rate of dissolution and the rate of surface alterations of TiO_2. These interactions can result in variation of the pH of the solution. This issue is discussed in detail in a later section. The fact that the "steady-state" semicontinuous reactor operation with respect to the rate of H_2 production is nearly identical to that of the batch reactor, after a sufficient time of illumination, indicates that

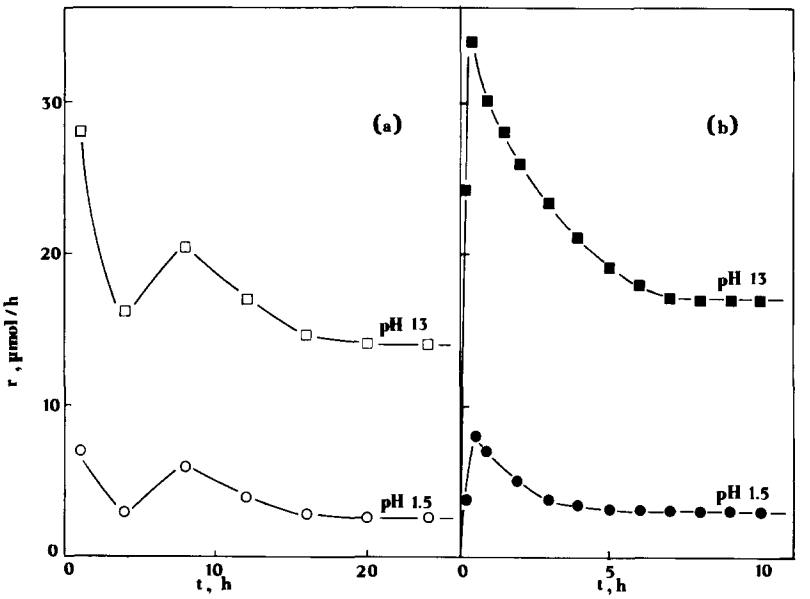

FIG. 2. Dynamic behavior of (a) a batch reactor and (b) a semicontinuous reactor operation with the 0.5% Pt–1% RuO_2 catalyst at two different pH levels.

the two systems stabilize at essentially the same state.

(*b*) *Influence of Stirring Speed on Rate of Hydrogen Production*

The influence of stirring speed on the rate of hydrogen production was investigated under both modes of reactor operation using the 1% Pt–1% RuO_2/TiO_2 catalyst prepared by method A at a pH of 13. Two catalyst loadings were used, 40 and 3 mg, under otherwise identical conditions. The "steady" rate of hydrogen production after a long period of illumination (approximately 20 h), is shown in Fig. 3 as a function of the stirrer speed. It is apparent in both cases, that the rate of H_2 production is a linear function of the stirrer speed, within the range of values employed in this investigation. The slope of the linear relationship seems to be a function of the catalyst loading. Thus, in the case in which 40 mg of catalyst was used, the slope is 8.5×10^{-3} μmol/h-rpm while in the case in which 3 mg of catalyst was used the slope is 3.5×10^{-3} μmol/h-rpm.

The enhancement of hydrogen production rate with stirrer speed is not due to elimination of mass transport resistances, as expected in classical catalytic systems, since such considerations do not apply in this particular case. The enhancement of H_2 production rate is probably due to increased uniformity of the slurry and increased frequency of exposure of the catalyst particles to light. The catalyst particles that are not in the illuminated side of the cell, or not close to its surface, receive light of reduced intensity due to absorption by water and primarily by other catalyst particles. As stirring increases, the frequency with which the catalyst particles pass through the illuminated side of the cell increases. When the catalyst particles are exposed to light, the electron excitation within TiO_2 occurs, while H_2 production, which is a "dark" reaction, occurs when the catalyst particles are removed from the illuminated side of the cell. Thus, the rate of H_2 production is directly proportional to the frequency of this cycle, which, in turn, is proportional to the stirrer speed. This explains the linear relationship between H_2 production rate and

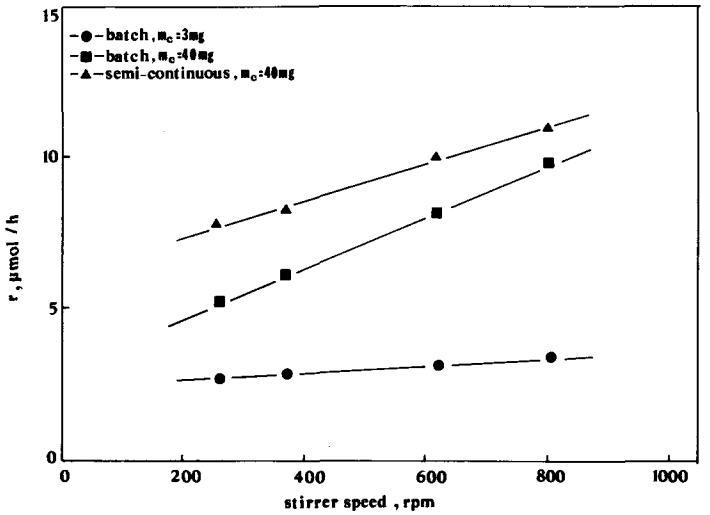

FIG. 3. Influence of stirrer speed on rate of hydrogen production in a batch or semicontinuous photoreactor for catalyst loadings of 3 and 40 mg.

stirrer speed observed in Fig. 3. The linear relationship is expected to hold until the frequency of the cycle approaches the frequency of the reaction.

When the catalyst loading is small (3 mg) the rate of H_2 production is not very sensitive to stirrer speed, as shown in Fig. 3. This is due to the fact that at low catalyst loadings the solution is much more transparent and thus nearly all particles are irradiated with approximately the same intensity. Thus, stirring is of reduced importance, as long as it is sufficient to maintain the catalyst particles in suspension.

The influence of stirrer speed on the rate of H_2 production in a semicontinuous reactor operation is also shown in Fig. 3 for a catalyst loading of 40 mg. In this type of operation the degree of agitation provided by the stirrer influences the rate of reaction less strongly than in the case of the batch reactor operation. The slope of the linear relationship is 6×10^{-3} μmol H_2/h rpm. The reduced influence of stirrer speed in the case of the semicontinuous operation is due to the fact that N_2 purging already provides agitation to the slurry. The extra agitation provided by the stirrer improves the operation for the same reasons as those discussed in the batch reactor operation. However, in this case, the relative enhancement of the H_2 production rate is smaller.

(c) *Influence of Catalyst Loading on Rate of H_2 Production*

To investigate the effects of catalyst loading on the rate of hydrogen production, a series of batch experiments were conducted with the 1% Pt–1% RuO_2/TiO_2 catalyst, in which the catalyst loading was varied between 2.5 and 85 mg. In all cases the pH was adjusted to 1.5 and all other parameters were identical. The steady rate of hydrogen production (r) is shown in Fig. 4 as a function of catalyst loading. The rate increases with catalyst loading, but not in a linear fashion, especially at low catalyst loadings, as would be expected. Furthermore, the rate of H_2 production per unit mass of catalyst (r_m), also shown in Fig. 4, decreases with catalyst loading. This quantity would have been expected to be independent of catalyst loading, resulting in a straight horizontal line in Fig. 4.

To provide an explanation for this discrepancy, the intensity of irradiation at the

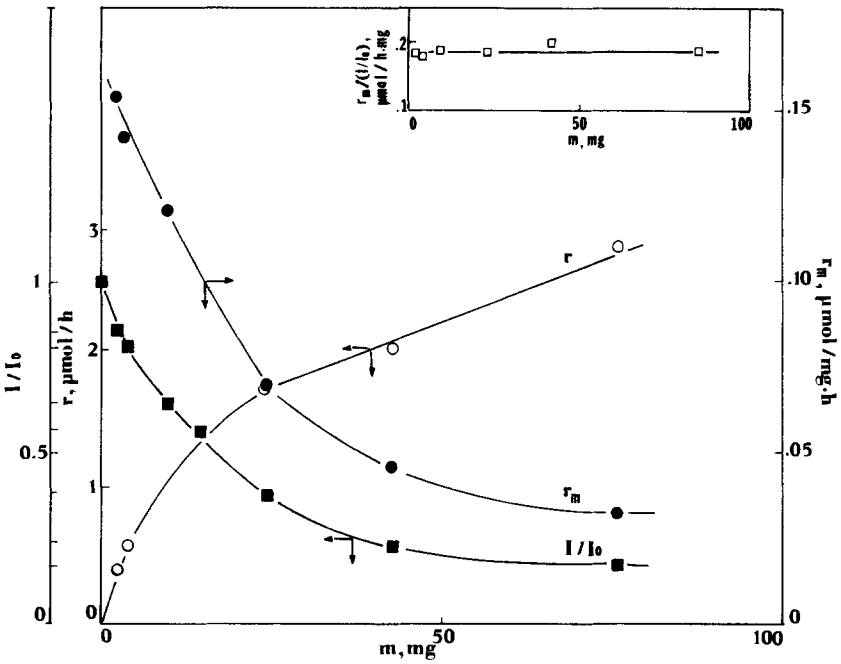

FIG. 4. Influence of catalyst loading on measured rate of H_2 production (r), rate per unit mass of catalyst (r_m), and normalized intensity at reactor cell outlet (I/I_0). Insert: Intensity-normalized rate as a function of catalyst loading.

outlet of the reactor cell was measured as a function of catalyst loading and the normalized intensity, I/I_0 (measured intensity at the reactor cell outlet divided by the intensity at the same point at zero catalyst loading), is also plotted as a function of catalyst loading in Fig. 4. It is obvious that the normalized intensity curve follows quite closely the curve of the rate per unit mass of catalyst. Thus, it can be concluded that the reduction in the rate of H_2 production per unit mass of catalyst is due to reduced transparency of the reaction slurry caused by increased concentration of catalyst particles. This conclusion implies that the rate of H_2 production per unit mass of catalyst per "unit transmission," which can be quantified by the parameter I/I_0, should be independent of catalyst loading. This is indeed the case, as is shown in the insert of Fig. 4, in which the parameter $(r_m)/(I/I_0)$ is plotted versus catalyst loading, resulting in a straight horizontal line.

This observation clearly shows that the mass of the catalyst alone is not sufficient to define specific rates of hydrogen production in photocatalytic systems. The transparency of the reaction slurry, which is affected by catalyst loading, plays an important role in the definition of the specific reaction rate. The parameter I/I_0 can be used to quantify this role and the true intrinsic rate could be expressed in the form of $(r_m)/(I/I_0)$.

This formulation of specific reaction rate in photocatalytic systems, combined with the finding that at low catalyst loadings the rate is nearly independent of stirrer speed, can be used in the comparison of the performance of different catalyst formulations or in the study of the effects of operational variables on measured reaction rates.

(*d*) *Influence of Catalyst Parameters on Rate of H_2 Production*

Parameters related to the formulation and to physical characteristics of catalysts can

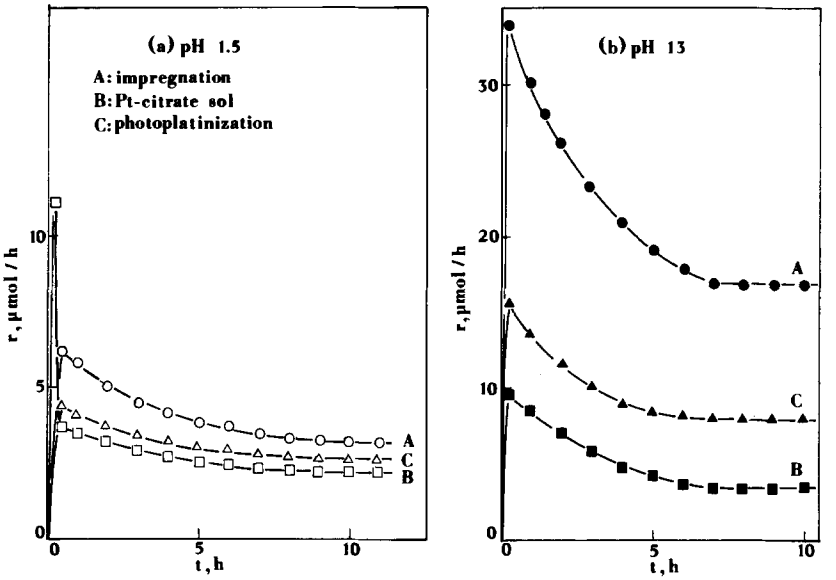

FIG. 5. Effects of catalyst preparation methodology on rate of hydrogen production at a pH of (a) 1.5 and (b) 13. (A) Incipient wetness impregnation, (B) Pt–citrate sol formation, (C) photoplatinization. All catalysts contain 0.5% Pt and 1% RuO_2.

play an important role in the definition of specific activity of certain reactions. In the present study, the influence of these parameters on the rate of hydrogen production was investigated employing three different catalyst preparation techniques and by varying the Pt loading, the average Pt crystallite size, and the temperature of reduction.

Results pertaining to three catalyst preparation procedures, incipient wetness impregnation (A), Pt–citrate sol formation (B), and photoplatinization (C) are presented in Fig. 5. A 0.5% Pt–1% RuO_2/TiO_2 catalyst was prepared in all cases. The catalysts were tested at two pH levels, 1.5 and 13, under otherwise identical conditions employing the semicontinuous photoreactor. The results of Fig. 5a, which pertain to a pH of 1.5, show that, after the systems have stabilized, the three catalyst formulations differ only slightly in the rate of hydrogen production. The incipient wetness impregnation technique gives a rate approximately 27% higher than the rate offered by the Pt–citrate sol formation technique and 13% higher than the rate offered by photoplatinization. However, in the initial stages of the reaction, and in particular during the first half hour, method B offers a rate that is significantly higher than that of method A. The reason for the dramatic drop of activity of the catalyst prepared by the Pt–citrate sol formation technique is not known. A plausible explanation is that the catalyst particles prepared with this technique are very finely dispersed but that under irradiation they agglomerate to larger particles with a concomitant drop in activity. Another explanation might be leaching of Pt crystallites from the TiO_2 carrier. Because Pt is precipitated on the TiO_2 surface, it is not expected to form strong adsorption bonds with its surface. Thus, a fraction of it could leach out within a short period of time.

Differences in the rate of H_2 production induced by the different preparation techniques are more pronounced when the photolysis is carried out at a pH of 13, as Fig. 5b indicates. Thus, catalysts prepared by

the incipient wetness impregnation technique offer rates approximately 75% higher than those offered by catalysts prepared by the Pt–citrate sol formation technique and 60% higher than the rates offered by catalysts prepared by the photoplatinization technique. The fact that the rate of H_2 production is enhanced at higher pH has been established in this work (see also Fig. 2 and Section (e)) and by other investigators (*10*). Figure 5, however, implies that the degree of sensitivity of the H_2 production rate depends on the catalyst preparation technique. This is probably due to structural and chemical differences induced on TiO_2 by the different catalyst preparation methodologies. The method of platinization of TiO_2 could influence the surface properties of TiO_2 such as surface charge and surface acidity/basicity characteristics, which in turn could affect the rate of H_2 production.

A number of catalyst formulations with variable Pt loading between 0 and 4 wt% were prepared on 1% RuO_2/TiO_2 support and tested under identical conditions at pH values of 1.5 and 13 in a batch photoreactor. The results, presented in Fig. 6 in the form of hydrogen production rate as a function of Pt loading, indicate that under both pH conditions the optimum Pt loading of the catalyst is in the neighborhood of 0.5 wt%. However, this is a weak optimum, especially at low pH. The free metallic surface area of Pt and the mean diameter of the Pt crystallites were also determined and are shown in Table 1. The mean crystallite sizes ranged between 4 and 14 Å. It is apparent from Fig. 6 that the rate of H_2 production is independent of Pt loading when this exceeds 1 wt% and is therefore independent of available Pt area. It is also interesting to observe that hydrogen is produced in the absence of Pt, which has also been observed by other investigators (*24, 25*). The presence of Pt in the catalyst formulation enhances the rate of H_2 production by a factor of 2 to 2.5, independent of the pH level.

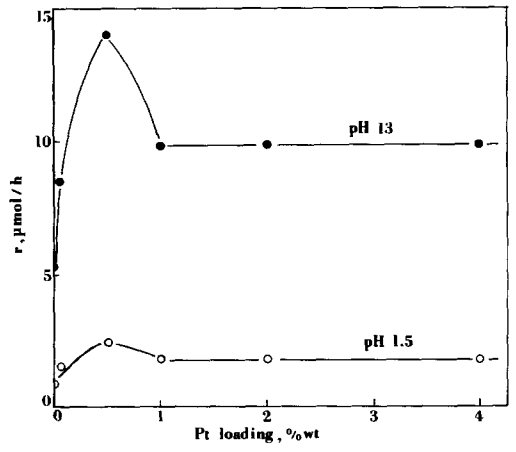

FIG. 6. Influence of Pt loading on x% Pt–1% RuO_2/TiO_2 catalysts on rate of H_2 production at two different pH levels.

TABLE 1

Free Metallic Surface Area and Mean Pt Crystallite Size of Pt/TiO_2 Catalysts Prepared by Incipient Wetness Impregnation

Pt loading (wt%)	S_{Pt} (m^2/g)	d (Å)
0.05	0.26	4
0.5	1.52	7
1	2.38	9
2	3.90	11
4	6.08	14

Concerning the mechanism of the process, the independence of the rate of H_2 production on Pt loading and available Pt area beyond a certain value implies that in this region the rate is controlled by the number of electrons that are excited in the semiconductor particles and that the probability of these electrons ending up in Pt crystallites is independent of the number of such crystallites available, after a critical number corresponding to approximately 1 wt% Pt has been achieved.

Another possible explanation of this phenomenon is offered by the work of Kiwi (*26*) who measured the concentration of Ti^{3+} cations on the TiO_2 surface as a function of Pt loading and found this to increase up to a Pt loading of approximately 0.5% and then

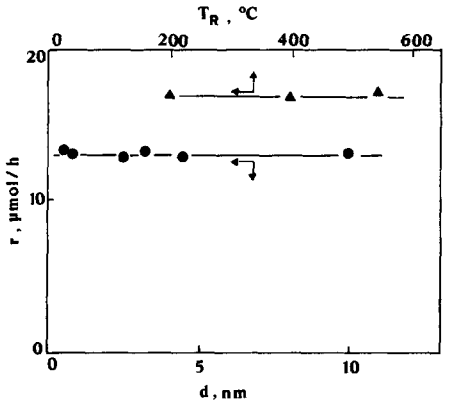

FIG. 7. Influence of mean Pt crystallite size and temperature of reduction on rate of hydrogen production in a semicontinuous photoreactor at a pH of 13.

stabilize. A closer examination of the two explanations reveals similar features since the concentration of Ti^{3+} cations is closely associated with the photogenerated electrons according to

$$TiO_2 + h\nu \rightarrow h^+_{TiO_2} + e^-_{TiO_2}(Ti^{3+}). \quad (4)$$

The existence of an optimum metal loading of 0.5 wt% is in good agreement with the work of Kiwi and Grätzel (*10*). An explanation for the observed optimum metal loading was sought in structural factors of the Pt crystallites, as related to the size of the crystallites. However, as discussed below, this does not provide an explanation for the observed metal loading.

To investigate the influence of Pt dispersion, or mean Pt crystallite size, on the rate of H_2 production, the 0.5% Pt/TiO_2 catalyst was sintered in air at various temperatures between 200 and 500°C and for a variable period of time. The resulting mean Pt crystallite sizes, as measured by hydrogen chemisorption after reduction, ranged between 6 and 100 Å. The rate of H_2 production obtained with the continuous flow reactor at a pH of 13 is shown in Fig. 7 as a function of the average Pt crystallite size.

It is apparent that the rate of H_2 production is independent of the size of the Pt crystallites or of the details of surface structure of the metallic surface. Therefore, it can be concluded that the photocatalytic water cleavage is a structure-insensitive or facile reaction, as far as Pt is concerned. It is also apparent from Fig. 7 that the rate of H_2 production is also independent of the available Pt area, a conclusion that is in agreement with earlier results of this study.

The results shown in Figs. 6 and 7 clearly demonstrate that the rate of hydrogen production is independent of phenomena occurring on the exposed Pt surface. This includes the rate of desorption of hydrogen from the catalyst surface. If the desorption of hydrogen was rate controlling, then the measured rate of H_2 production would be expected to depend on the available Pt area. Figures 6 and 7 demonstrate that this is not the case. The rate of H_2 production could also be controlled by physical phenomena such as H_2 mass transfer from liquid to gas phase. Evidence against this is provided by comparing the results of the batch and semicontinuous experiments, under otherwise identical conditions. If mass transfer were rate controlling, then a significantly higher rate would be expected under semicontinuous reactor operation since, in this case, the liquid–gas interfacial area is much larger than in the batch case due to the presence of dispersed gas bubbles in the liquid phase. However, as Fig. 2 shows, nearly identical H_2 production rates were measured under both reactor operations.

The independence of the rate of the photocatalytic water cleavage on the size of the metal crystallites, on the available Pt area, and on the population of the Pt crystallites, at least beyond a certain metal loading, can be explained evoking the theory of metal–semiconductor contacts. According to this theory the Fermi levels of a metal and a semiconductor in contact and at thermodynamic equilibrium are at equal heights. This requirement results in electron transfer between the two solids, the direction of which depends on the initial (before contact) work function of the two solids. In the particular case of $Pt–TiO_2$, the work function

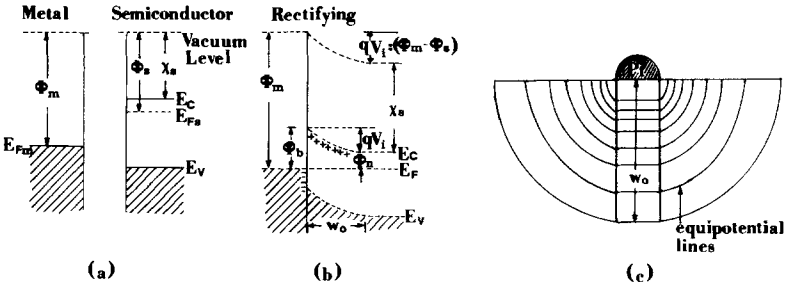

FIG. 8. Electron energy band diagram of a metal in contact with an *n*-type semiconductor with $\Phi_m > \Phi_s$. (a) Neutral materials separated from each other. (b) Thermal equilibrium situation after contact has been made. (c) Equipotential line distribution in the electron depletion region of the semiconductor. E_c and E_v are the conduction band minima and valence band maxima, E_{Fm} and E_{Fs} are the metal and semiconductor Fermi levels, respectively, q is the electron charge, V_i is the contact potential, and χ_s is the electron affinity.

of Pt (Φ_m) is higher than that of TiO_2 (Φ_s). The electron energy band diagram of a metal in contact with an *n*-type semiconductor with $\Phi_m > \Phi_s$ is shown in Fig. 8 for (a) neutral materials separated from each other and (b) the equilibrium situation after contact has been made. In this situation a Schottky barrier of magnitude Φ_b develops. The conduction band electrons that cross over into the metal leave a positive charge of ionized donors behind, so that a region in the semiconductor of depth W_0 near the metal becomes depleted of mobile electrons. Thus, a potential distribution develops within this region of the semiconductor, as shown in Fig. 8c in which equipotential lines are shown. The potential distribution is represented by the density of the equipotential lines. It is assumed that the potential is zero in the neutral bulk region of the semiconductor. Details of these developments have been reported elsewhere (*27*).

The photogenerated electrons are attracted into the potential well developed as discussed above near the metal–semiconductor interface and cross over into the Pt particle by thermionic emission or by quantum-mechanical tunneling/field emission (*28*). If it is assumed that the rate-controlling step of the entire photocatalytic water cleavage process is the photoelectron excitation in TiO_2, then the rate of hydrogen production would indeed be independent of the population of the Pt particles on the TiO_2 surface, after a critical surface density (or Pt loading) has been achieved and also independent of the size of the Pt crystallites. Alternatively stated, the photocatalytic water cleavage is not a process dependent on surface phenomena but on phenomena occurring in the bulk of the solid semiconductor. This explains the insensitivity of the process to the magnitude of the available Pt surface area after a critical value has been established. However, it does not explain the weak maximum observed at the 0.5% Pt loading of the catalysts, as shown in Fig. 6.

A final parameter, related to the preparation of the catalysts, which was investigated, is the temperature of reduction. The 0.5% Pt–1% RuO_2/TiO_2 catalyst was prepared following the incipient wetness impregnation technique and it was reduced at various temperatures between 200 and 520°C. The results shown in Fig. 7 demonstrate that the rate of H_2 production is independent of the temperature of reduction. This is probably due to the fact that complete reduction of Pt occurs at 200°C and due to the general insensitivity of the process to parameters related to the structural details of the metallic component of the catalyst.

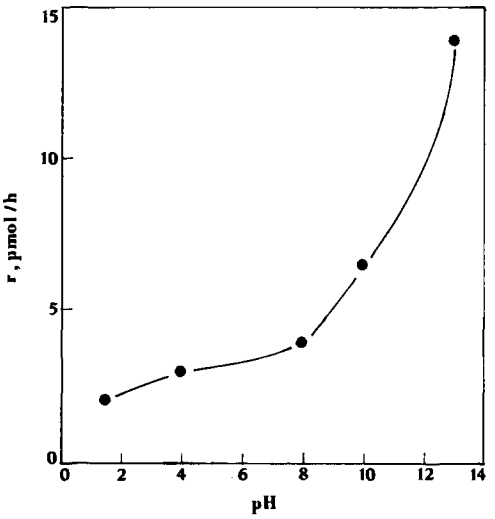

FIG. 9. Effects of pH of suspension on rate of H_2 production in a batch photoreactor. The 0.5% Pt–1% RuO_2 catalyst is used.

(e) *Influence of pH on Rate of H_2 Production*

The influence of the pH of the suspension on the rate of H_2 production was investigated in batch experiments employing the 0.5% Pt–1% RuO_2/TiO_2 catalyst. The pH was adjusted to the desired value by addition of either NaOH or HCl. The results in the form of the steady rate of hydrogen production are shown in Fig. 9. It is apparent that high pH values favor H_2 production whose rate increases rapidly at a pH >10. The results presented in Fig. 9 are in general agreement with those reported by Kiwi and Grätzel (*10*) for a Pt/TiO_2 catalyst.

The enhancement of the rate of H_2 production at higher pH levels is probably due to increased concentration of physisorbed OH^- groups at higher pH values. The primary step in the water cleavage process under near-UV illumination is the generation of electron-hole pairs in the semiconductor, according to Eq. (4). These two species may recombine in the bulk lattice or migrate to the surface where they can react with adsorbates. Recombination can be avoided if the two species are separated and subsequently trapped by appropriate sites. Hole trapping is carried out by surface hydroxyl groups (OH_s^-), a process which is assisted by physisorbed hydroxyl groups (OH_p^-). Surface hydroxyl groups interact with positive holes resulting in the formation of hydroxyl radicals ($OH_s^\cdot$), according to (*29–31*)

$$OH_s^- + h^+ \rightarrow OH_s^\cdot. \qquad (5)$$

Surface hydroxyl radicals, in turn, interact with physisorbed hydroxyl groups to produce surface hydroxyl groups and physisorbed hydroxyl radicals according to

$$OH_s^\cdot + OH_p^- \rightarrow OH_s^- + OH_p^\cdot. \qquad (6)$$

Therefore, physisorbed OH^- ions act as charge carrier species, participating in a process of charge transfer between the semiconductor and the electrolyte (*29*).

From the above consideration it is apparent that OH^- ions participate in the hole trapping process, thus permitting the photogenerated electrons to reach the Pt sites. Higher pH implies higher concentration of OH^- ions and therefore higher rate of H_2 production by the photocatalytic water cleavage process.

It must be pointed out that the pH values shown in Fig. 9 correspond to the adjusted, initial values. It was observed that during the course of the reaction the pH of the suspension varied with time. This is illustrated in Fig. 10 in which the variation of both pH and rate of hydrogen production with time of illumination is shown for three different initial catalyst particle sizes. It must be pointed out, however, that under identical conditions but without illumination (therefore no reaction) the pH of the suspension dropped from its initial value of 10 to a value of 9.8 upon addition of the catalyst and remained unchanged with time. It is apparent from Fig. 10 that the variation of the rate of H_2 production with time follows very closely the variation of pH with time. This is indeed an expected result in view of the discussion above and of the results presented in Fig. 9. Figure 10, however, indi-

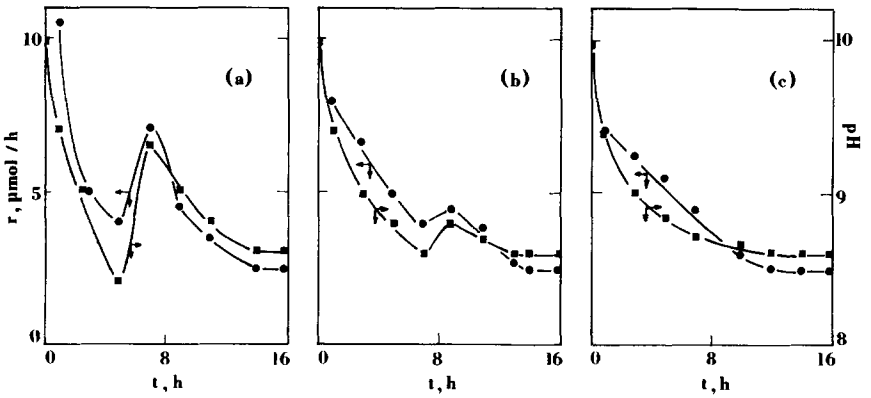

FIG. 10. Variation of pH and rate of H_2 production with time for three different catalyst particle sizes: (a) $d_p > 0.4$ mm, (b) $0.4 < d_p < 0.125$ mm, (c) $d_p < 0.063$ mm. The 0.5% Pt–1% RuO_2/TiO_2 catalyst was used in all cases.

cates that the dynamic behavior, in terms of pH and rate of H_2 production, depends on the initial size of the catalyst particles. This is probably due to the fact that the larger catalyst aggregates break up under stirring and as a result of increased surface area or alteration of surface charge, the adsorption of OH^- ions is enhanced, leading to decreased pH of the slurry. The decreased pH leads to reduced rates of hydrogen production. The local maxima observed with the medium and large size particles cannot be easily explained with the available information. Finally, it must be pointed out that at steady conditions (after many hours of illumination) the three systems stabilize at essentially the same pH and rate of hydrogen production. In this state the particle size distribution was measured by a laser particle counter and found to be nearly identical for all three systems.

(*f*) *Dependence of H_2 Production Rate on the Intensity of Illumination*

The dependence of H_2 production rate on the intensity of illumination was investigated using the 450-W and the 1000-W Xe lamps whose outlet intensity could be varied within limits. The intensity of illumination of the lamps was measured at wavelengths between 250 and 400 nm. H_2 production rates over the 1% Pt–1% RuO_2/TiO_2 catalyst were determined in the batch reactor at a pH of 13, as a function of the illumination intensity. The results are shown in Fig. 11 in terms of the measured intensity at the lamp outlet, reported as percentage based on the measured maximum intensity at the 1000-W setting. The results show a linear relationship between the rate of H_2 produc-

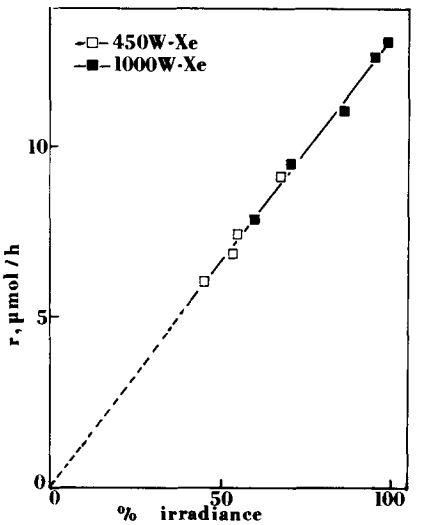

FIG. 11. Influence of intensity of illumination on rate of H_2 production in a batch photoreactor. A 450-W and a 1000-W Xe lamp were used.

tion and the intensity of illumination within the stated range of wavelengths. It is interesting to observe that the experimental points of both lamps define the same line, indicating that, under otherwise identical conditions, the rate of H_2 production is only a function of the intensity of illumination in the UV.

The linear relationship between H_2 production rate and light intensity is due to the proportionality between light intensity and number of photons emitted within the same range of frequencies. Every photon absorbed by the catalyst generates an electron-hole pair according to

$$TiO_2 + h\nu \rightarrow TiO_2\,(e^-, h^+). \quad (7)$$

The electron is transferred to a Pt crystallite where the dark reaction takes place:

$$Pt(e^-) + H^+OH \rightarrow \frac{1}{2} H_2 + OH^- + Pt. \quad (8)$$

Thus, two electrons are required for the production of a hydrogen molecule, and the rate of H_2 production is expected to be proportional to the rate of photon generation or otherwise to the intensity of the illumination.

However, not all electrons generated result in hydrogen production since a fraction of these recombine with the positive holes. The fact that the linear relationship between H_2 production rate and illumination intensity holds over the entire range of intensities implies that the frequency of e^-/h^+ recombination also increases linearly with intensity, within the range of intensities investigated. This implies that higher illumination intensities can be utilized without sacrificing efficiency due to enhanced e^-/h^+ recombination.

It was argued in Section (d) that the rate of hydrogen production is independent of surface phenomena and that it only depends on the number of electrons that are excited in the semiconductor. Figure 11 provides additional evidence that the rate-controlling step is the electron excitation process, which, as discussed above, depends on the intensity of illumination. However, as discussed in Section (c), the intensity of illumination alone cannot define an intrinsic rate for hydrogen production since the photon flux within the cell is affected by operational variables. This problem is resolved by incorporation of the relative intensity, I/I_0, within the definition of the intrinsic rate.

CONCLUSIONS

The following conclusions can be drawn from the results of this study of photocatalytic water cleavage over a Pt–RuO_2/TiO_2 catalyst under near UV illumination.

(a) An intrinsic rate of hydrogen production, at a given pH level, can be defined if it is expressed per unit mass of catalyst per unit transmission.

(b) The rate of hydrogen production is independent of the details of surface structure of Pt; it shows a weak maximum at a Pt loading of 0.5 wt%, and is independent at Pt loadings exceeding 1 wt%. However, the rate is dependent on the method of platinization of TiO_2, especially at high pH levels.

(c) The rate of H_2 production is strongly dependent on the pH of the suspension. The enhancement of the rate with increasing pH becomes more pronounced when the pH exceeds 10.

(d) The rate of photocatalytic water cleavage is a linear function of the intensity of illumination in the near UV.

ACKNOWLEDGMENTS

The authors express their gratitude to Professors Pizanias and Koutsoukos for many valuable discussions.

REFERENCES

1. Harriman, A., and West, M. A., "Photogeneration of Hydrogen." Academic Press, New York, 1982.
2. Grätzel, M., Ed., "Energy Resources through Photochemistry and Catalysis." Academic Press, New York, 1983.
3. Kalyanasundaram, K., Borgarello, E., and Grätzel, M., *Helv. Chim. Acta.* **64,** 362 (1981).
4. Kudo, A., Tanaka, A., Domen, K., Maruya, K. I., Aika, K. I., and Onishi, T., *J. Catal.* **111,** 67 (1988).

5. Domen, K., Naito, S., Onishi, T., and Tamaru, K., *Chem. Phys. Lett.* **92,** 433 (1982).
6. Somorjai, G. A., Hendewerk, M., and Turner, J. E., *Catal. Rev.–Sci. Eng.* **26,** 683 (1984).
7. Sato, S., and White, J. M., *J. Phys. Chem.* **85,** 592 (1981).
8. Duonghong, D., and Grätzel, M., *J. Chem. Soc., Chem. Commun.*, 1597 (1984).
8. Borgarello, E., Kiwi, J., Pelizzetti, E., Visca, M., and Grätzel, M., *Nature* **289,** 158 (1981).
10. Kiwi, J., and Grätzel, M., *J. Phys. Chem.* **88,** 1302 (1984).
11. Bard, A. J., *J. Phys. Chem.* **86,** 172 (1982).
12. Mills, A., and Porter, G., *J. Chem. Soc., Faraday Trans. 1* **78,** 3659 (1982).
13. Kiwi, J., and Grätzel, M., *J. Phys. Chem.* **90,** 637 (1986).
14. Kiwi, J., and Morrison, C., *J. Phys. Chem.* **88,** 6146 (1984).
15. Borgarello, E., Kiwi, J., Pelizzetti, E., Visca, M., and Grätzel, M., *J. Am. Chem. Soc.* **103,** 6324, 1981.
16. Borgarello, E., Kiwi, J., Grätzel, M., Pelizzetti, E., and Visca, M., *J. Am. Chem. Soc.* **104,** 2996 (1982).
17. Yesodharan, E., and Grätzel, M., *Helv. Chim. Acta.* **66,** 2145 (1983).
18. Munuera, G., Fernandez, A., and Espinos, J. P., *in* "2nd E.E.C. Workshop on Photochemical and Photobiological Processes for Producing Energy-rich Compounds, Carmona, Sevilla, 1987," p. 97.
19. Yoneyama, H., Nishimura, N., and Tamura, H., *J. Phys. Chem.* **85,** 268 (1981).
20. Duonghong, D., Borgarello, E., and Grätzel, M., *J. Am. Chem. Soc.* **103,** 4685 (1981).
21. Escudero, J. C., Cervera-March, S., Giménez, J., and Simarro R., *J. Catal.* **123,** 319 (1990).
22. Escudero, J. C., Giménez, J., Simarro, R., and Cervera-March, S., *Sol. Energy Mater.* **17,** 151 (1988).
23. Mills, A., *J. Chem. Soc., Chem. Commun.*, 367 (1982).
24. Keller, P., Moradpour, A., and Amouyal, E., *J. Chem. Soc., Faraday Trans. 1* **78,** 3331 (1982).
25. Amouyal, E., Keller, P., and Moradpour, A., *J. Chem. Soc., Chem. Commun.*, 1019 (1980).
26. Kiwi, J., *J. Phys. Chem.* **90,** 1493 (1986).
27. Akubuiro, E. C., and Verykios, X. E., *J. Catal.* **103,** 320 (1987); *J. Catal.*, **113,** 106 (1988).
28. Tyagi, M. S., *in* "Metal-Semiconductor Schottky Barrier Junctions and Their Applications" (B. L. Sharma, Ed.), Plenum, New York, 1984.
29. Salvador, P., *J. Electrochem. Soc.* **128,** 1895 (1981).
30. Enea, O., Ali, A., and Duprez, D., *New J. Chem.* **12,** 27 (1988).
31. Turchi, C. S., and Ollis, D. F., *J. Catal.* **122,** 178 (1990).